The Effect of Geometry on the Acoustic Radiation of Plasma Filaments in Air

Konstantinos Kaleris, Yannis Orphanos, Makis Bakarezos, Nektarios Papadogiannis, John Mourjopoulos

The effect of plasma geometry on the acoustic radiation of laser filaments

Konstantinos Kaleris[1] Yannis Orphanos[2,3] Makis Bakarezos[2,3] Nektarios Papadogiannis[2,3] and John Mourjopoulos[1]

[1] Audio & Acoustic Technology Group, Wire Communications Laboratory, Dept. of Electrical and Computer Engineering, University of Patras, Rion Campus 26504, Greece

[2] Department of Music Technology & Acoustics, Hellenic Mediterranean University, 74133 Perivolia, Rethymnon, Greece

[3] Institute for Plasma Physics and Lasers, Hellenic Mediterranean University, 74100 Tria Monastiria, Rethymnon, Greece

kkaleris@upnet.gr

ABSTRACT

Laser-generated plasma filaments in ambient air generate acoustic pulses with characteristic emission directivity and frequency spectra. This work studies the effect of the geometrical characteristics of the plasma channel on the generated acoustic radiation. For this purpose, a model based on the classical line source is adopted, which deploys the correlation between light and sound following laser breakdown to predict the acoustic radiation of filaments in air. Through the model, the acoustic directivity and frequency spectra of plasma filaments with different lengths and plasma density distributions are studied. Preliminary results from acoustic measurements of the filament's sound radiation are presented in the frequency domain. Finally, a complete model based on the wave equation with a heat source is outlined, which allows for the estimation of the filament's acoustic radiation in the time and frequency domain at any point in space. Preliminary results from a computational simulation of a scaled model of a plasma channel are also shown, indicating that such a model can predict the directivity and spectral characteristics of filament sound sources.

1. INTRODUCTION

Gas ionization from short or ultrashort laser pulses (Laser Induced Breakdown – LIB) has attracted interest in recent years as it is suitable for various scientific and technological applications. LIB is followed by secondary radiative phenomena, particularly the emission of light originating from electron recombinations, de-excitations and heat, as well as the emission of sound generated by the thermoelastic expansion of the interaction volume that leads to the formation of pressure at the boundary with the surrounding air. A well-established technique deploying these secondary radiative phenomena is LIB Spectroscopy (LIBS), in which, elemental analysis is achieved by measuring the spectrum of the plasma luminescence or the acoustic spectrum of the shock wave following breakdown [1][2]. LIB is also investigated as a method for controlling meteorological phenomena by remote generation of plasma filaments in the atmosphere [3][4], for medical applications [5] and for military / defense applications [6]. LIB has also been proposed as a novel transduction mechanism for the formation of massless and spatially unbound acoustic sources with controlled directivity [7][8][9]. Recently, the possibility of modulating the LIB acoustic pulses in order to generate continuous and controlled sound for direct reproduction of complex audio signals, such as speech and music, has also been demonstrated [10].

Light-matter interaction causing breakdown in ambient air has been experimentally studied since the early 1960s [11]. For sufficient laser pulse intensity, part of the optical energy is absorbed by the air particles producing a free electron density. The initially cold ions in the plasma volume gain energy through interactions with the free electrons and move radially out of the plasma core, causing a localized thermoelastic expansion. From the expansion, pressure is generated at the boundary of the ionization volume with the surrounding air particles that leads to the emission of a shock wave, which progressively transforms into a sound wave in the source's far field [12]. LIB shock waves have the time signature of N-waves with a duration in the order of microseconds and pressure that can exceed 130dB, depending on the characteristics of the optical pulse. The acoustic energy of the LIB pulses extends from the low frequencies of the audible range up to the ultrasounds, as shown in Fig.1.

Apart from the generation of the sound wave, LIB is followed by the emission of light due to Bremsstrahlung, electron transitions (including radiative recombinations and de-excitations) and heating [12][13]. At times comparable to the laser pulse duration, when the electron density in the interaction volume is high, secondary plasma radiation originates mainly from free-free transitions of decelerating electrons (Bremsstrahlung) [14]. At early times after the laser pulse excitation, light radiation is produced mainly from electron-ion recombinations (free-bound transitions) [14] and radiative electron de-excitations (bound-bound transitions). Thermal radiation due to heating also starts to develop because of the progressive energy transfer from the electrons to the ions, atoms and molecules in the interaction volume. Finally, at the later stages, radiation is emitted mainly due to thermal phenomena and electron de-excitations, until the air

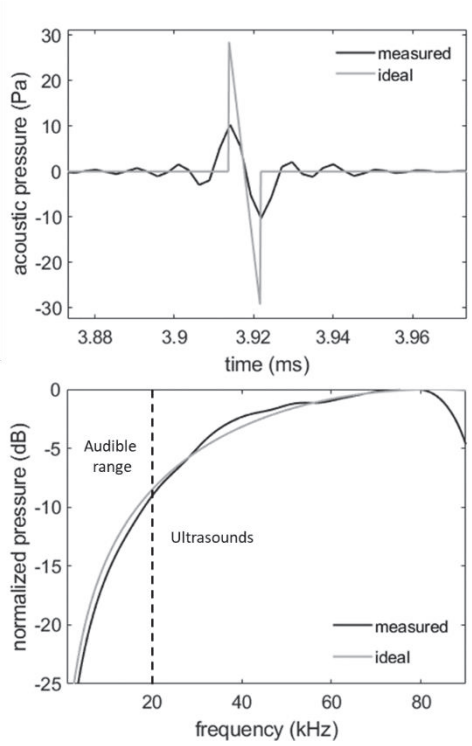

Figure 1: a) time- and b) frequency-domain representations of typical measured and ideal acoustic N-wave generated by a 23fs, 5.4mJ laser pulse (from [15] - modified).

molecules cool down to ambient temperature. These radiative processes are reflected in the time-resolved light signal emitted from the interaction volume during the process. Such an optical signal captured by a photodiode is shown in Fig. 2. A conceptual chain of the process behind laser-induced breakdown in air is shown in Fig. 3. Laser filaments in air are a special type of laser-generated plasma sound sources, which are of particular interest for acoustics applications due their inherent emission directivity. Laser filaments are elongated plasma threads generated during non-linear propagation of ultrashort laser pulses with sufficient energy to evoke self-focusing effects. Self-focusing is the result of the change in the refractive index of a material in response to the electric field of the laser pulse (Kerr effect). In the air, it takes place only with ultrashort laser pulses (picosecond, femtosecond), due to the very high optical power required. When ultrashort laser pulses are loosely focused in the air by a lens with a small numerical aperture, the combined action of self-focusing and defocusing, due to diffraction and plasma defocusing, lead to recurrent tightening and broadening of the plasma channel along the pulse propagation axis, as shown in Fig. 3. The acoustic emission of such a cylinder-like plasma sound source exhibits a characteristic directivity, in analogy to that of an acoustic line source or a line array [15].

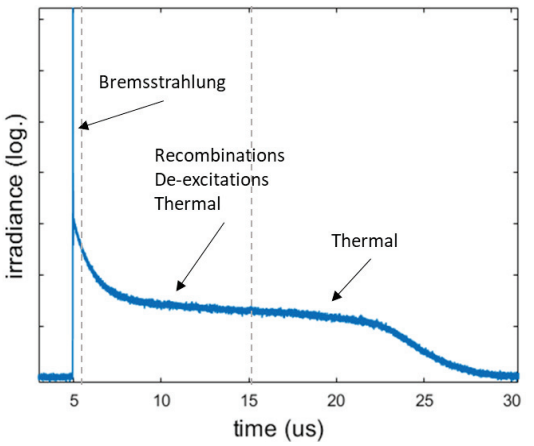

Figure 2: light signal emitted during LIB captured by a shown (from [17] – modified).

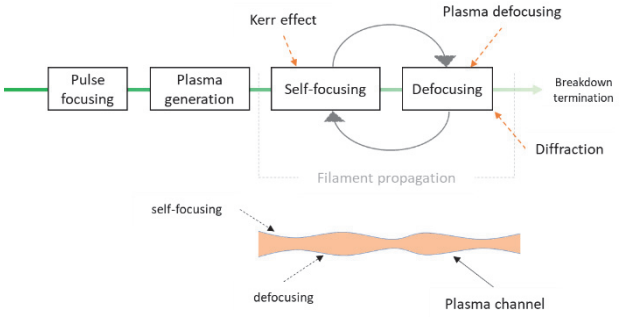

Figure 4: the physical mechanisms behind filament propagation of an ultrashort laser pulse.

In a previous work, it has been demonstrated that the directivity of a filament acoustic source can be predicted from the acoustic line source model by using the axial distribution of the light irradiance as a pressure weighting factor along the filament's axis. Here, the line source model is used to study the effect of the length and of the initial axial pressure distribution of the plasma channel on the sound directivity of the filament source. Moreover, a

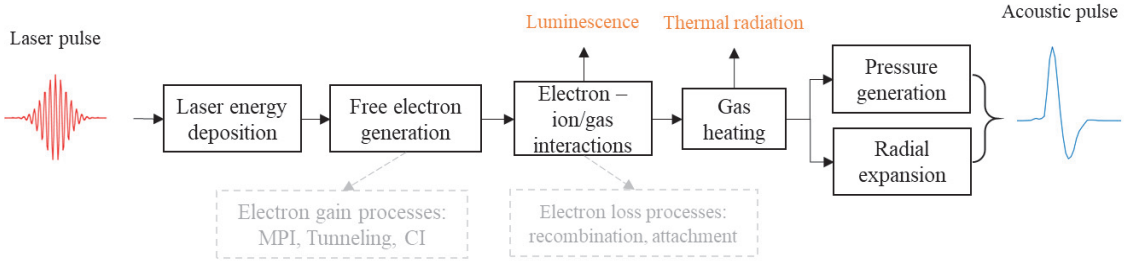

Figure 3: conceptual chain of processes behind laser-induced breakdown in air

new physical model is proposed for calculating the filament's acoustic radiation at any point in space within or beyond the audible frequency range, utilizing the heat source model of laser-driven sound generation [photo]. In this approach, the time evolution of the heat flow in the interaction volume is approximated via a Gaussian function, in accordance to the experimental results presented in [16].

2. ESTIMATING SOUND FROM LIGHT IN LASER-INDUCED BREAKDOWN

As described in the previous section, sound generation in laser-induced gas breakdown is the result of the thermoelastic expansion of the ionized volume. Hence, laser-driven sound generation can be attributed to the heat flow in and out of the light-air interaction volume. Moreover, it is well known that the heat flow rate is proportional to the irradiance of the thermal radiation from the heated volume. It becomes evident that the generated acoustic wave can be predicted by the heat flow rate in the interaction volume as estimated from the measurement of the thermal radiation. Suppose a sphere S with radius R centered at the origin of a spherical coordinates system. representing the air volume where the laser energy is deposited. The sphere is positioned inside an infinite reservoir corresponding to the surrounding air. In this scenario, the plasma source is generated under tight focusing, where the resulting plasma geometry is spherical. The increase in thermal energy inside the sphere results to acoustic pressure due to the thermoelastic expansion. Thus, the generation and propagation of the pressure wave in the air can be described by a wave equation with a heat source term [17][17]. For the purpose of this work, the non-linearities due to supersonic expansion velocities are neglected and thus, the pressure $p(r,t)$ at a distance r and time t generated by the heat source is written as:

$$\left(\nabla^2 - \frac{1}{c^2}\frac{\partial^2}{\partial t^2}\right)\cdot p(r,t) = -\frac{\gamma-1}{c^2}\cdot\frac{\partial}{\partial t}H(r,t) \tag{1}$$

where c is the speed of sound, $\gamma = \frac{c_p}{c_v}$, where c_P, c_V the specific heat capacity of the air under constant pressure and constant volume respectively, and $H(r,t)$ is the rate of heat evolution per unit volume. Using the Fourier transform, we get:

$$\left(\nabla^2 - \frac{\omega^2}{c^2}\right)\cdot p(r,\omega) = i\omega\frac{(\gamma-1)}{c^2}H(r,\omega) \tag{2}$$

The solution of Eqn. (2) in the far field takes the form:

$$p(r,\omega) = \pi\omega\frac{(\gamma-1)}{c^2}\cdot H_0^{(1)}(kr)\cdot\int_0^R J_0(k\rho)\,H(\rho,\omega)\rho d\rho \tag{3}$$

where $H_0^{(1)}(kr)$, $J_0(k\rho)$ are the zero-order Hankel and Bessel functions respectively, k the wave number, r the distance from source and ω the angular frequency.

In LIB, the air heating is a secondary phenomenon resulting from the interactions of the free electrons with the ions and gas molecules. Thus, the source term of Eqn. (1) has to be adapted appropriately to describe such a heating. Due to the complexity of the involved phenomena that make this task extremely challenging the heat source profile is estimated here estimated from the thermal radiation of the heated volume [16]. The rate of heat transfer $H(t)$ between the sphere and the bath can be evaluated from the inward and outward radiation $P_{in}(t)$ and $P_{out}(t)$ emitted from the sphere to the surrounding environment:

$$H(t) = P_{out}(t) - P_{in}(t) \tag{4}$$

Assuming that the thermal radiation follows the Stefan-Boltzmann law for the Blackbody radiation with emissivity equal to one[1] we get:

$$\begin{aligned} P_{in}(t) &= \sigma A(t) T_{air}^4, \\ P_{out}(t) &= \sigma A(t) T_S^4(t) \end{aligned} \tag{5}$$

where σ the Boltzmann constant, A the surface of the boundary between the sphere and the surrounding air, T_S the temperature of the sphere and T_{air} the room temperature.

By definition, the temperature T_{air} of the reservoir remains constant during the phenomenon, thus only T_S is a function of time. The surface of the boundary $A(t)$ is also a function of time, since the heating causes the sphere to expand. Substituting P_{in} and P_{out} into Eqn. (4), the rate of heat transfer becomes:

$$H(t) = \sigma A(t)(T_S^4(t) - T_{air}^4) \tag{6}$$

It should be mentioned that the thermal radiation of the air at room temperature ($T_{air} = 300K$) is beyond the wavelength range of the measuring photodiode. As a result, the thermal signal $s_H(t)$ received by the photodiode can be approximately considered to be proportional to $T_S^4(t)$. The emitted thermal radiation signal $s_H(t)$ can be written as:

$$s_H(t) = b\cdot H(t) = b\sigma A(t) T_S^4(t) \tag{7}$$

where b is a scaling factor. Taking the Fourier transform of Eqn. (7) we get:

[1] The emissivity value is not significant here, as the model is normalized and constant factors are neglected.

$$H(\omega) = \int_{-\infty}^{\infty} H(t) \cdot e^{-i\pi\omega t} = \frac{1}{b} S_H(\omega) \tag{8}$$

Moreover, the radial distribution of the heating function can be approximated by the radial distribution of the laser pulse intensity [17][18]. In this case, the heat distribution follows a Gaussian shape in the radial dimension, such that:

$$S_H(r, \omega) = e^{i\omega c(r)} \cdot e^{-\frac{r^2}{2R^2}} \cdot S_H(\omega) \tag{9}$$

where $c(r)$ is a function of the radial distance from the center of the volume. Finally, by substituting the heat term of Eqn. (8) and (9) into Eqn. (3) and by neglecting any constant factors, we get:

$$p(r, \omega) = \omega \cdot H_0^{(1)}(kr) \cdot \int_0^R J_0(k\rho) \cdot S_H(\rho, \omega) \cdot \rho d\rho \tag{10}$$

Eqn. (10) gives the normalized frequency spectrum of the LIB acoustic wave after propagating for a distance r away from source. It has been demonstrated that presented model can be used for precise evaluations of the frequency spectrum of acoustic pulses generated by nanosecond laser pulses under tight focusing conditions. This model will be used as the basis for the development of a physical model of the sound radiation of laser plasma filaments.

3. LINE SOURCE MODEL OF THE FILAMENT ACOUSTIC RADIATION

As described in the Introduction, the acoustic radiation of plasma filament has been described using an adapted acoustic line source model. Here, the basic concept behind the model are presented. It is known that the acoustic pressure $p(r, \phi, t)$ reaching a point (r, ϕ) on the polar plane at time t, generated by an acoustic line source of length L consisting of elementary point sources arranged one next to the other on the x axis, is given by:

$$p(r, \phi, t) = \int_{-L/2}^{L/2} \frac{H_x(x)}{r'(x)} \cdot n\left(t - \frac{r'(x)}{c}\right) dx \tag{11}$$

where $H_x(x)$ is the axial pressure distribution along the axis x of the source, $r'(x)$ is the distance of an elementary source residing at point x from the listener:

$$r'(x) = \sqrt{\left(cos\,\phi - \frac{x}{r}\right)^2 + (sin\,\phi)^2}$$

and $n(t)$ is the pressure excitation function of the elementary sources. Laser-generated acoustic pulses can be effectively modeled through triangular N-shaped pulses:

$$n(t) = -\frac{t}{T} \cdot [u(t+T) - u(t-T)]$$

where $u(t)$ is the unit step function and T is the half of the pulse [15]. This model is used here to evaluate the directivity and frequency spectrum of plasma filaments with different geometrical characteristics. Moreover, it is used as reference for comparison with the predictions of the proposed physical model.

4. PHYSICAL MODEL OF THE FILAMENT SOUND RADIATION

In this section, the development of a complete model is investigated by re-writing the wave equation model presented in Section 2 in the two-dimensional space. Eqn. (1) becomes:

$$\left(\nabla^2 - \frac{1}{c^2}\frac{\partial^2}{\partial t^2}\right) \cdot p(x, y, t) = -\frac{\gamma - 1}{c^2} \cdot \frac{\partial}{\partial t} H(x, y, t) \tag{12}$$

Here, the heat source $H(x, y, t)$ is expressed in terms of three distinct functions:

$$H(x, y, t) = H_x(x) \cdot H_y(y) \cdot H_t(t) \tag{13}$$

where $H_x(x)$ and $H_y(y)$ are the distribution of heat flow along the x and y axis and $H_t(t)$ is the function representing the time evolution of the heat flow. From [15] it is known that the axial distribution of the heat flow can be approximated by a Lorentzian function:

$$H_x(x) \sim \frac{1}{1 + (x/\gamma)^2} \tag{14}$$

where 2γ is the Full-Width at Half-Maximum (FWHM). Moreover, as presented before, the distribution on the radial dimension can be considered to be Gaussian:

$$H_y(y) \sim e^{-\frac{y^2}{2\sigma_y^2}} \tag{15}$$

with σ_y the width parameter.

For the requirements of the qualitative study presented here, the absolute magnitude of the heat flow rate is not of interest and will be normalized. Under these assumptions, the heat source is finally written as:

$$H_t(x, y, t) = \frac{1}{1 + (x/\gamma)^2} \cdot e^{-\left(\frac{y^2}{2\sigma_y^2} + \frac{t^2}{2\sigma_t^2}\right)} \tag{16}$$

and eq. (12) becomes:

$$\left(\nabla^2 - \frac{1}{c^2}\frac{\partial^2}{\partial t^2}\right) \cdot p(x, y, t) = \frac{\gamma - 1}{\left(1 + \left(\frac{x}{\gamma}\right)^2\right) c^2 \sigma_t} t e^{-\left(\frac{y^2}{2\sigma_y^2} + \frac{t^2}{2\sigma_t^2}\right)} \tag{17}$$

Eqn. (17) is solved numerically in MATLAB [19] and the results are shown in the next section.

5. RESULTS

5.1 Frequency spectra

In this subsection, preliminary results from acoustic measurements of the filament sound radiation are presented. The experiments were carried out at the laboratories of the Institute for Plasma Physics and Lasers of the Hellenic Mediterranean University in Rethymnon, Crete. Fig.5 shows the experimental setup used for the acoustic measurements. The filament was generated by a Ti:Sapphire laser (Amplitude Technologies, Evry, France) with 23 fs optical pulses at Full Width at Half Maximum (FWHM), center wavelength λ = 800 nm and pulse energy

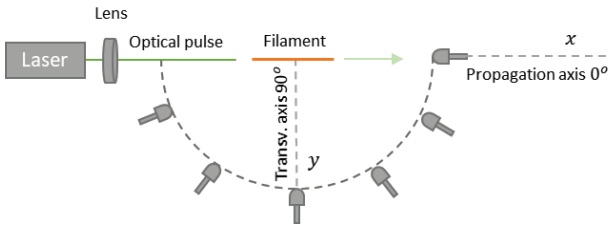

Figure 5: experimental setup for acoustic measurements of the filament's sound radiation.

Ep = 5.4 mJ. The pulses were focused using a lens with focal length of 120 cm (f/48).

The luminescence of the plasma channel used as the initial pressure profile $H_x(x)$ of the acoustic source, was captured by a CCD camera and was analyzed with image processing techniques to extract the distribution of the light irradiance along the filament's axis. In this case, the Lorentzian distribution parameter a takes the value $\gamma = 0.0149$ m and the FWHM of the plasma filament is 3.2 cm while the total length of the source is approximately 14 cm. The acoustic signals were recorded using a GRAS 46BF-11/4 in. microphone (GRAS Sound & Vibration A/S, Holte, Denmark) with a GRAS 12AA power module and the data were acquired by an RME Fireface 802 sound card (Audio AG, Haimhausen, Germany) at 192 kHz sampling rate and 24 bits resolution, allowing for a measurement bandwidth of about 90 kHz. The measurements at different positions around the source were carried out at a step of approximately 20°, keeping a constant distance of 30 cm from the center of the plasma. This distance is sufficient to capture the far field radiation of the sound source.

Fig.6 presents the normalized spectral magnitude of the plasma filament acoustic radiation in different angles from the propagation axis. It becomes evident that the filament's radiation is stronger on the transverse axis while it becomes weaker as we move towards the pulse propagation axis. Additionally, the frequency spectrum of the emitted sound at 90^o resembles that of an N-pulse (see Fig. 1) while with decreasing angle, spectral dips appear in the higher end of the spectrum. These dips are characteristic of comb filtering, which essentially is the result of frequency-dependent constructive and destructive

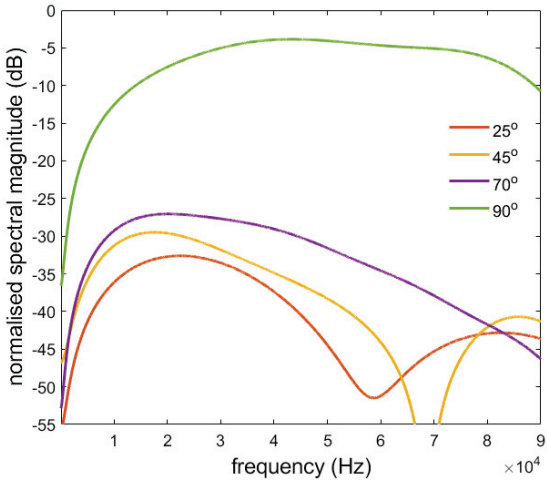

Figure 6: indicative measured frequency spectra of the filament's acoustic radiation at different angles.

interferences of sound waves emitted from the contributing elementary sources.

Fig. 7 shows the normalized spectral magnitude of the filament's acoustic radiation at 25^o from the filament's axis, as evaluated from the acoustic measurements and the

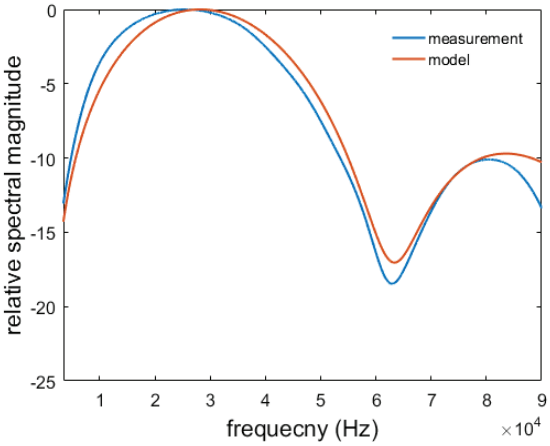

Figure 7: measured and calculated normalized frequency spectra of the filament's acoustic radiation at 25^o.

model. It can be seen that the matching between the model's prediction and the measurement is very good.

5.2 Acoustic directivity

In this subsection, the directivity of the filament's acoustic radiation is evaluated in terms of the geometry of the plasma thread. The study is carried out via the acoustic line source model presented in Section 3 and investigates the impact of:

a. the length,
b. the axial distribution $H_x(x)$

of the plasma channel in the filament's acoustic directivity. From [20] it can be seen that the light irradiance in laser filaments can have a bell-shaped or flat-top axial distribution. In order to identify the impact of the different $H_x(x)$ on the acoustic directivity of laser filaments, two such plasma channels of $L = 14$cm length are simulated, one with a Lorentzian (see Eqn. ()) and one with a 6th-order

super-Gaussian axial distribution. For reasons of comparison, the total irradiance represented by:

$$I_{tot} = \int_{-L/2}^{L/2} H_x(x)dx$$

is kept constant for the two cases. This is achieved by using a variance parameter of the super-Gaussian $\sigma_{SG} = 0.0187$. The simulation results are shown in Fig. 8a. For the directivity plots, only the energy within the audible bandwidth 20Hz-20kHz is considered.

Moreover, Fig. 8b shows the directivity plots for four filaments of different lengths at 70cm distance from the filament's center. The axial distribution $H_x(x)$ is scaled appropriately to account for the change in the filament's total length. The filament lengths and FWHM are shown in Tab. 1.

Length (cm)	FWHM (cm)
3.5	0.8
7	1.6
14	3.2
28	6.4

Table 1: full length and FWHM of the simulated plasma channels.

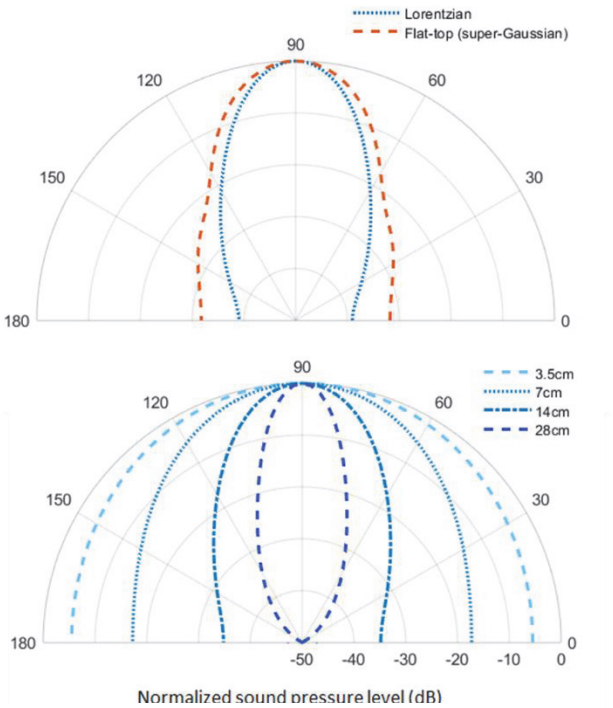

Figure 8: directivity plots in the audible spectrum evaluated at 70cm distance from the filament's center for a) two filaments of 14cm length and different axial pressure distributions and b) four filaments with lengths 3.5cm, 7cm, 14cm and 28cm.

From the polar plots it becomes evident that the filament's acoustic emission becomes strongly directional with increasing length of the plasma channel. For the 28cm plasma channel, there is almost no acoustic emission in the direction of the filament axis, while the 3.5cm plasma source exhibits almost omnidirectional emission.

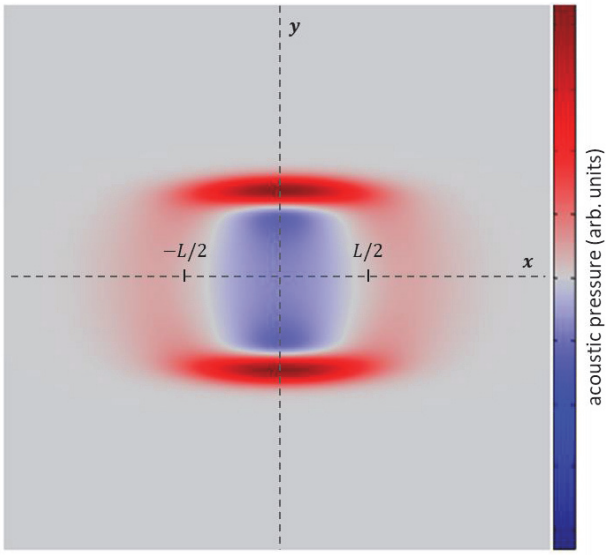

Figure 9: pressure generated by a plasma filament at the early stages of the thermoelastic expansion, simulated via the physical model.

5.3 Preliminary evaluations of the physical model

In this subsection, preliminary results from evaluations of the acoustic radiation of laser filament sound sources through the physical model described in Section 4 are presented. To simplify the computational evaluations, the filament model is scaled in time and space and the results are shown in arbitrary units; nevertheless, they demonstrate the characteristic features of the filament acoustic radiation, and particularly the directivity and the dips in the spectral magnitude. Fig. 9 shows a heat map of the pressure generated by a plasma filament at the early times after the thermoelastic expansion. As expected, high pressure is generated along the filament axis and propagates in the transverse direction, while the soundwave propagating towrads the x direction is weak. This is in accordance with the results of Fig. 6 and Fig. 8.

Moreover, Fig. 10 shows the frequenncy-domain representation of the filament's acoustic pressure as obtained from the model at 3 different angles. Again, the sound pressure is stronger on the transverse axis y ($\varphi = 90^o$) while it fades for smaller angles with respect to the filament axis. Also, the frequency spectrum on the transverse axis is identical to that of an N-pulse, while at smaller angles, characteristic spectral dips appear. These qualitatively results are in accordance with Fig. 6, however, for precise matching with the acoustic line source model and the experimental measurements, a real-scale physical model has to be developed.

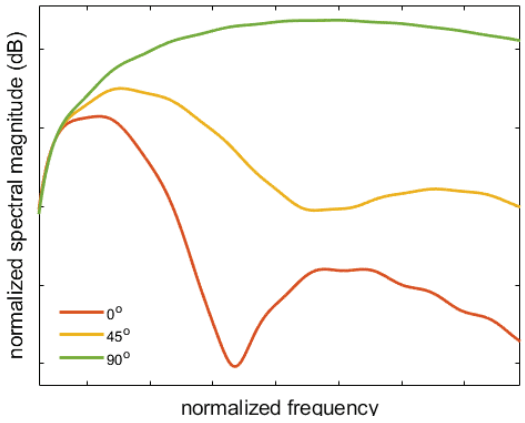

Figure 10: indicative acoustic frequency spectra of a plasma filament at different angles, calculated via the proposed physical model.

6. CONCLISIONS AND DISCUSSION

This work investigated the acoustic radiation of plasma filaments with respect to the geometrical characteristics of the plasma channel and particularly the initial pressure distribution along the filament's axis and the length of the channel. The study was carried out using the acoustic line source model for plasma filaments and focused on the audible frequency range of the acoustic radiation. For the pressure distributions, a Lorentzian function and a 6^{th}-order super-Gaussian function were used to represent bell-shaped and flat-top pressure distributions respectively. From the simulations it was demonstrated that the acoustic radiation of filaments with a flat-top distribution is less directional than that of filaments with a bell-shaped distribution. Also, longer plasma channels were found to exhibit stronger acoustic directivity in the far field, while the plasma source becomes omnidirectional in the acoustic frequency range for plasma channels in the order of a few centimeters.

Moreover, a physical model was proposed for the evaluation of the acoustic radiation of plasma filaments in the time and frequency domain. The model is based on the heat source model for laser-generated sound sources that allows for the evaluation of the sound radiation of such sources in air from the light irradiance originating from secondary radiative phenomena taking place in LIB. Preliminary qualitative results from a scaled physical model of a plasma channel were presented, showing the capability of the model to predict the directivity and spectral characteristics of laser filaments.

In this respect, the origins of the comb filtering effect on the frequecy spectrum of the filament acoustic radiation that leads to spectral dips has to be further investigated in the future. The proposed model is suitable for such a study since by changing the fineness of the grid, the heat source can become either a continuous line or a discontinuous line array. Moreover, precise acoustic measurements have to be carried out for laser filaments of different lengths and axial distributions, to validate the predictions of the acoustic line source model and to be used as reference for the development of the complete physical model.

7. REFERENCES

[1] Shah, S. K. H., Iqbal, J., Ahmad, P., Khandaker, M. U., Haq, S. & Naeem, M. Laser induced breakdown spectroscopy methods and applications: A comprehensive review, Radiation Physics and Chemistry, 170, 108666 (2020).

[2] Jolivet, L., Leprince , M., Moncayo, S., Sorbier, L., Lienemann, C.-P. & Motto-Ros, V. Review of the recent advances and applications of LIBS-based imaging, Spectrochimica Acta Part B: Atomic Spectroscopy, 151, 41-53 (2019).

[3] Papeer, J., Botton, M., Gordon, D., Sprangle P., Fibich, G., Herzig Sheinfux, H., Zigler A. & Henis, Z. Multi variable control of filamentation of femtosecond laser pulses propagating in air. Journal of Physics B: Atomic, Molecular and Optical Physics 48, 094005 (2015).

[4] Henis, Z., Milikh, G., Papadopoulos, K. & Zigler, A. Generation of controlled radiation sources in the atmosphere using a dual femtosecond / nanosecond laser pulse. Journal of Applied Physics 103, 103111 (2008).

[5] Killiny, N., Etxeberria, E., Flores, A. P., Blanco, P. G., Reyes, T. F., & Cabrera, L. P. Laser-induced breakdown spectroscopy (LIBS) as a novel technique for detecting bacterial infection in insects. Scientific Reports 9 (2019).

[6] Jones, T., Hornstein, M., Ting, A. & Wilkes, Z. Intense underwater laser acoustic source for Navy applications. The Journal of the Acoustical Society of America 125, 2556-2556 (2009).

[7] Gómez Bolaños, J., Delikaris-Manias, S., Pulkki, V., Eskelinen, J. & Hæggström, E. Laser-induced acoustic point source for accurate impulse response measurements within the audible bandwidth. The Journal of the Acoustical Society of America 135, EL298-EL303 (2014).

[8] Gómez-Bolaños, J., Delikaris-Manias, S., Pulkki, V., Eskelinen, J., Hæggström, E. & Jeong, C.-H. Benefits and applications of laser-induced sparks in real scale model measurements. The Journal of the Acoustical Society of America 138, EL175-EL180 (2015).

[9] Hornstein, M., Jones, T., Ting, A. & Nicholas, M. Directivity and frequency control of an intense underwater laser acoustic source for navy applications. The Journal of the Acoustical Society of America 127, 1985-1985 (2010).

[10] Kaleris, K. Stelzner, B., Hatziantoniou, P., Trimis, D. & Mourjopoulos, J. Laser-Sound: optoacoustic transduction from digital audio streams, Nature Scientific Reports (accepted manuscript) (2020).

[11] Nelson, P., Veyrie, P., Berry, M. & Durand, Y. Experimental and theoretical studies of air breakdown by intense pulse of light. Physics Letters 13, 226-228 (1964).

[12] Zel'dovič, J. & Rajzer, J. *Physics of shock waves and high-temperature hydrodynamic phenomena*. (Acad. Pr., 1970).

[13] Hamam, K., Gaabour, L. & Gamal, Y. Numerical modeling for investigating the optical breakdown threshold of laser-induced air plasmas at different laser characteristics. Physics of Plasmas 24, 073515 (2017).

[14] Chen, J., Ni, X., Lu, J., & Bian, B. Initial formation process of laser-induced plasma shock wave in air. Optics Communications, 176(4-6), 437-440 (2000).

[15] Kaleris, K., Orfanos, Y., Bakarezos, M., Papadogiannis, N. & Mourjopoulos, J. Experimental and analytical evaluation of the acoustic radiation of femtosecond laser plasma filament sound sources in air. The Journal of the Acoustical Society of America 146, EL212-EL218 (2019).

[16] Kaleris, K., Orphanos, Y., Bakarezos, M., Dimitriou, V., M., Tatrakis, M., Mourjopoulos, J. & Papadogiannis, N. On the correlation of light and sound radiation following laser-induced breakdown in air, Journal of Physics D: Applied Physics (2020).

[17] Diebold, G. J. “Application of the Photoacoustic Effect to Studies of Gas Phase Chemical Kinetics”, *Topics in Current Physics Vol.46: Photoacoustic, Photothermal and Photochemical Processes in Gases*, edited by Peter Hess, Springer, (1989).

[18] Couairon, A. & Mysyrowicz, A. Femtosecond filamentation in transparent media, Physics Reports, Volume 441, Issues 2–4, Pages 47-189, (2007).

[19] MATLAB. 9.7.0.1190202 (R2019b). Natick, Massachusetts: The MathWorks Inc. (2019).

[20] Point, G. Energy deposition in air from femtosecond laser filamentation for the control of high voltage spark discharges, PhD thesis, Laboratoire d’Optique Appliquée, Ecole Polytechnique, Palaiseau, France (2015).

ACKNOWLEDGEMENT

Author Konstantinos Kaleris acknowledges the support of his work by both the General Secretariat for Research and Technology (GSRT) and the Hellenic Foundation for Research and Innovation (HFRI). Authors Yannis Orfanos, Makis Bakarezos and Nektarios Papadogiannis acknowledge support of this work by the project "ELI - LASERLAB Europe Synergy, HiPER & IPERION-CH.gr" (MIS 5002735) which is implemented under the Action “Reinforcement of the Research and Innovation Infrastructure", funded by the Operational Programme "Competitiveness, Entrepreneurship and Innovation" (NSRF 2014-2020) and co-financed by Greece and the European Union (European Regional Development Fund).